

SWEDISH INSTITUTE OF SPACE PHYSICS

Space Environment Laboratory Work with SPENVIS



The Pichler-Hakenberg Orbit

by

Jan Hakenberg
Matthias Pichler

Referee: Dr. Johnny Ejemalm

Kiruna, 23th April 2007

Contents

Introduction	1
1 Mission characteristics	2
1.1 Orbital parameters	3
1.2 Characteristic Regions and their effects on the spacecraft	4
1.2.1 Auroral region	4
1.2.2 Inner van-Allen radiation belt	6
1.3 Low Earth orbit environment parameters	7
1.3.1 Compensation of drag	7
1.3.2 Surface charging	8
2 Effects of radiation	11
2.1 Flux of particles	11
2.2 Lifetime and performance degradation	14
2.2.1 Shielding of the solar array	14
2.2.2 Total dose in the memory device	16
2.2.3 Atomic oxygen erosion	17
2.2.4 Influence of glow on optical sensor	18
2.3 Single event upset	19
2.3.1 LET spectrum	19
2.3.2 Cross section and components characteristics	19
2.3.3 SEU rate estimation	21
Conclusion	24
Bibliography	25

Introduction

We devise a new orbit: the Pichler-Hakenberg orbit, which passes through the auroral region, the neutral environment in the LEO region, and the inner van-Allen radiation belt. The spacecraft that is assigned to the orbit, faces various environmental effects.

After making a preliminary estimate of the particle flux, we simulate the effects of the space environment using SPENVIS.

We compute the thickness of a layer of glass to reduce the electron equivalent fluence to a desired threshold. However, employing such a covering layer might contribute significantly to the total mass.

For protection of a memory device, we derive the thickness of shielding, to ensure the device is functioning during the entire mission.

We compute the amount of fuel required to compensate the drag encountered in the low altitudes.

We yield the spacecraft potential in altitudes below 2000 km, to investigate if charging is an issue in these altitudes.

A silver plate is mounted in the front of the spacecraft. The plate will be eroded due to atomic oxygen. We make a sophisticated guess on what the rate of erosion will be.

We derive if a sensitive CCD sensor needs to be covered during the passage of the auroral region to shield from glow.

The sensitivity function of the SMJ329C50GFAM66 memory component is modeled by a Weibull distribution function. A least-square fit to experimental data gives a good approximation to the parameters that define this distribution function.

We determine, which of four memory devices has the lowest single event upsets rate, and is therefore the most reliable to be used in space applications.

For simulation, modeling, and analysis of the spacecraft in the various space environments, we primarily query SPENVIS. As required, we develop small pieces of MATLAB code to perform numerical computations.

However, some of the extra work is carried out with the help of Mathematica.

Chapter 1

Mission characteristics

The Pichler-Hakenberg orbit has been designed to traverse through two major regions of interest.

- Auroral region
- Inner van-Allen radiation belt

The objective of the mission is to collect information on the particle distribution and the effect of the different space environments on the satellite. The mission duration is planned to be 5 years.

The launch is scheduled on the 17. September 2007 at 07:30 from Kourou in French Guiana, see Figure 1.1. The site is located approximately 500 km north of the equator, corresponding to a latitude of $5^{\circ}3'N$. In this region, the Earth's rotation gives an additional velocity of approximately 500 m/s, when the launch trajectory heads eastward. This circumstance makes the launch more cost efficient because the amount of fuel required is reduced.



Figure 1.1 : Launchsite in Kourou. Image is taken from <http://esamultimedia.esa.int>.

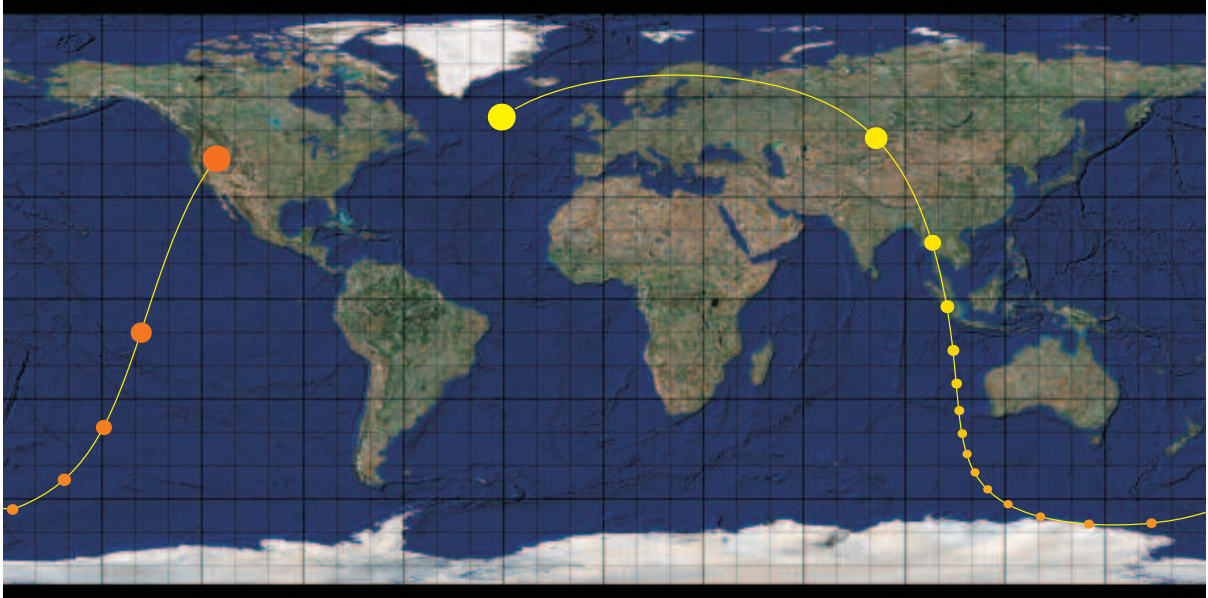


Figure 1.2 : Possible subsatellite track during one orbit. The size of the dots are inverse proportional to the altitude. The time elapse between two dots is 15 minutes. The track has been computed using Mathematica.

1.1 Orbital parameters

The Pichler-Hakenberg orbit is characterized by the following parameters:

Perigee altitude [km]	307.5
Apogee altitude [km]	15783.3
Inclination [deg]	67.5
Right asc. of asc. node [deg]	70.8
Argument of perigee [deg]	62.3
True anomaly [deg]	213.5

From these values, we compute an orbital period of

$$T = 17232.8s$$

Equivalently, we have exactly 5 orbits per siderial day. However, the orbit is not Earth synchronous.

Figure 1.2 shows a possible ground track of one orbital period. The time increment between two dots is 15 minutes.

A different plot, Figure 1.3, shows the spacecraft during 5 orbits in an Earth fixed coordinate system. The color code indicates the local time in the different time zones around the globe.

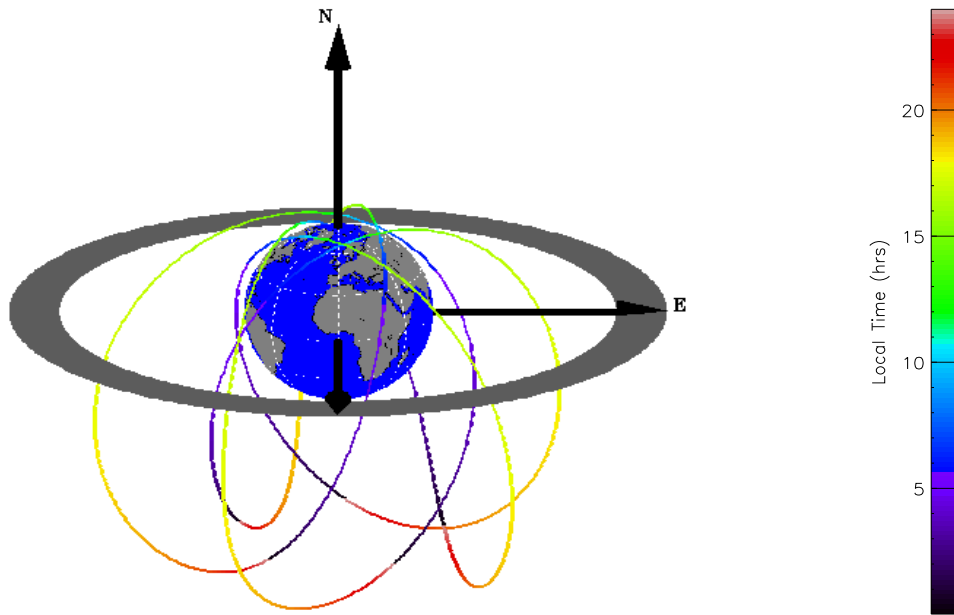


Figure 1.3 : 3D-view of the spacecraft during 5 orbits in the Earth fixed coordinate system. The image has been generated by SPENVIS.

Due to the comparably low altitude, the spacecraft leaves the magnetosphere at no time. The perigee is always close to the northpole and its apogee lays between the two van-Allen radiation belts. This can be seen in Figure 1.3. At the apogee region there is very low flux, however between the apogee and the perigee points a significant particle flux is encountered. This indicates two complete passages of the spacecraft through the inner van-Allen radiation belt per orbit.

1.2 Characteristic Regions and their effects on the spacecraft

The spacecraft orbit was carefully designed so that the spacecraft traverses the auroral region and the inner van-Allen radiation belt. These prominent space environments constantly influence the spacecraft during the mission.

1.2.1 Auroral region

The magnetic field of the Earth is modeled as a dipole depicted in Figure 1.4. The auroral regions are located around the two poles where the density of the magnetic field lines is greatest. In the magnetosphere, energetic charged particles are gyrating around the field lines, while oscillating

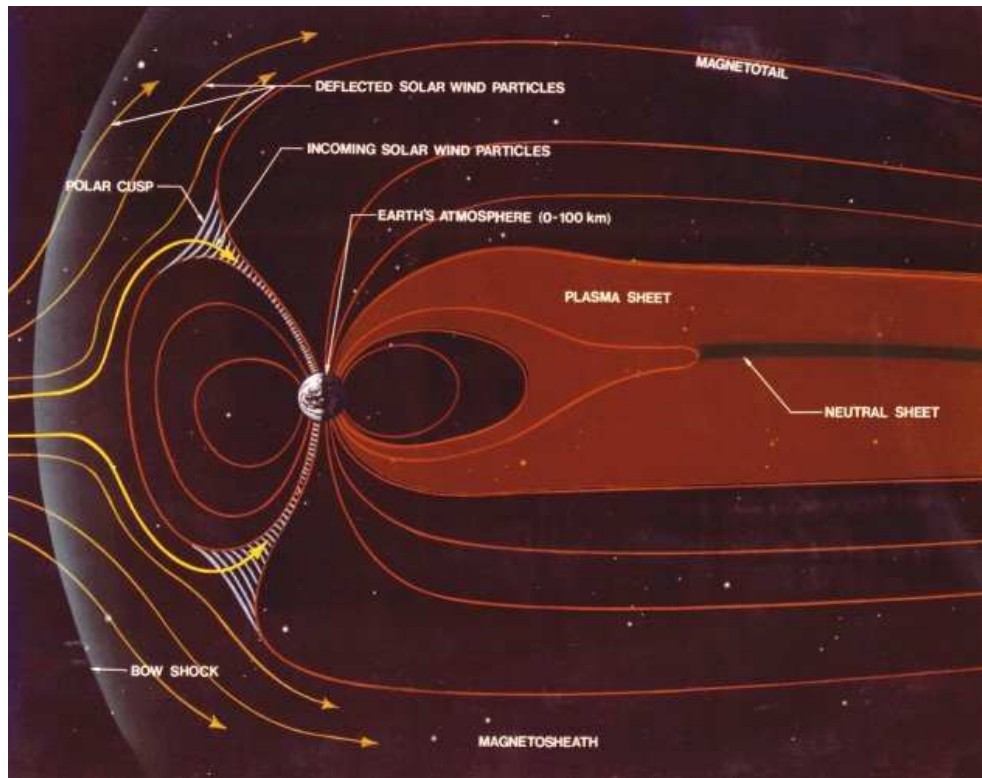


Figure 1.4 : The effect of the solar wind on the magnetic field of the Earth. The illustration is taken from en.wikipedia.org.

between the magnetic north and south pole. However, the graphic also suggests, that particles from the solar wind can immediately reach low altitudes.

Charged particles gyrating around the magnetic field lines in low altitudes are likely to collide with particles in the dense ionosphere. In the process of exciting electrons of the atoms in the ionosphere, photons will be emitted. During strong solar activity, this effect can be observed from the Earth surface as the auroral light. The different wavelengths of the auroral light reveal information about the space weather. Therefore, the auroral region is of interest for physicists.

The Pichler-Hakenberg orbit only meets the auroral region of the northern hemisphere. According to [La07], the boundaries of the auroral region are roughly given by

Latitude [deg]	65 – 75
Altitude [km]	80 – 1000

We take these boundaries as a guidance in calculations. By numerical simulation, we yield that the spacecraft spends 296.88s in the auroral region per orbit. This corresponds to 1.72% of the total orbit duration. The satellite passes through the region with an average speed of 9.30 km/s.

The most significant influence of the auroral region on the spacecraft are radiation effects. Even at low altitudes there are energetic particles, which interact with the spacecraft. This effects the

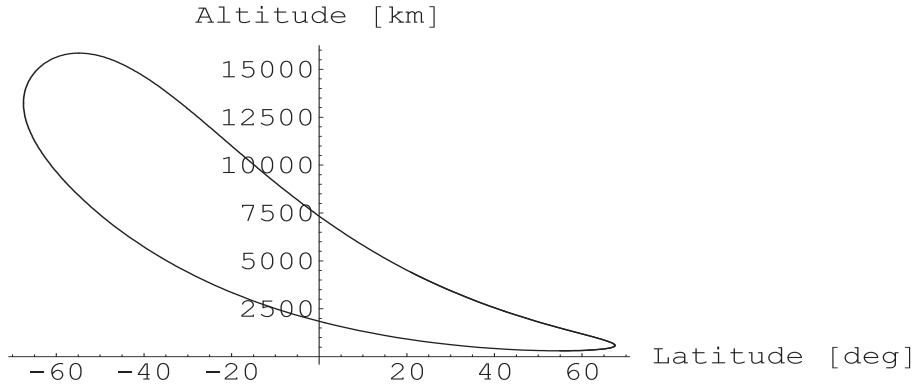


Figure 1.5 : Latitude vs. Altitude plot. The graphic has been computed using Mathematica.

electronics. Single event upsets rate are high, and spacecraft charging occurs. These properties are also encountered in equatorial medium and high earth orbits, that is in altitudes > 1000 km. The dominant particular species in the auroral region is atomic oxygen. We discuss erosion of a silver plate due to atomic oxygen in Section 2.2.3.

1.2.2 Inner van-Allen radiation belt

According to [WiRb07], the inner van-Allen belt ranges between $700 - 10000$ km altitude above the equatorial region. In different latitudes, the range in altitude varies with the alignment of the magnetic field lines.

Then, by numerical simulation we yield that the spacecraft spends $5233s$ in the inner van-Allen radiation belt per orbit. This corresponds to 30.4% of the total orbit duration. The satellite passes through the region with an average speed of 7.05 km/s.

The inner van-Allen belt contains high concentrations of energetic protons with energies > 100 MeV and electrons with energies $\simeq 400$ keV. These charged particles gyrate around the Earth's magnetic field lines.

A rotational symmetric potential function of the Earth's magnetic field is given by

$$B(r, \theta) = \frac{M_d}{r^3} \sqrt{3 \cos^2 \theta + 1} \quad \text{and} \quad M_d = 8 \cdot 10^{15} [Tm^3]$$

where r is the radial distance from the center of the Earth, and θ is the geomagnetic colatitude.

It is believed that protons of energies exceeding 50 MeV at lower altitudes are the result of the beta decay of neutrons created by cosmic ray collisions with nuclei of the upper atmosphere. The source of lower energy protons is proton diffusion due to changes in the magnetic field during geomagnetic storms.

The average energy level of electrons and protons in the belt is only of a few eV but there are also few high energetic particles in the order of MeV.

Due to the slight offset of the belts from Earth's geometric center, the inner van-Allen radiation belt is closest at the South Atlantic Anomaly. There, the inner radiation belt reaches altitudes as low as 250km at high solar activity.

At energy levels of MeV the energetic particles have sufficient energy to penetrate through the shielding of electronics and cause logic errors in the circuitry due to single event upset and latch-ups. The upsets are soft errors, because they do not cause permanent damage. The latch-ups seriously threaten the permanent functioning of the electronics.

Both types of errors might lead to a failure of a subsystem or even the loss of the mission. To avoid these consequences, the electronics have radiation hardness and the circuit design is adapted to deal with upsets and latch-ups.

In addition, shielding is placed around the sensitive areas but increases the weight of the spacecraft. This trade-off is discussed at the example of solar array in section ??.

1.3 Low Earth orbit environment parameters

A spacecraft on the Pichler-Hakenberg orbit, experiences altitudes between 307.5–15783.3 km. In this section, we investigate the environmental conditions encountered during the phase when the spacecraft is in the altitude range of 300–2000 km.

1.3.1 Compensation of drag

From [Ej07b], we know that the drag force computes as

$$D = \frac{1}{2}C_d A \rho v^2$$

for a constant C_d , the effective area of exposure A , ρ as the particle density, and v the velocity of the spacecraft.

The drag constant is of the general form

$$C_d = 2 \left((1 - \sigma) \cos^2(\theta) - (1 - \tau) \sin^2(\theta) + 1 \right)$$

For our spacecraft the values $\sigma = 0.6$, and $\tau = 0.2$ apply. Due to the shape of the spacecraft, we estimate $\theta = 10^\circ$. Thus, we yield a drag constant of

$$C_d = 2.72763$$

The effective area of exposure is estimated as $A = 20\text{m}^2$, to which the solar array contributes a huge fraction.

The decrease in impulse Δp due to drag during one orbit is determined by the expression

$$\Delta p = \int_0^T D(t) dt = 27.2763 \int_0^T \rho(t) v(t)^2 dt = 83.1608 \frac{\text{kg m}}{\text{s}} \quad (1.1)$$

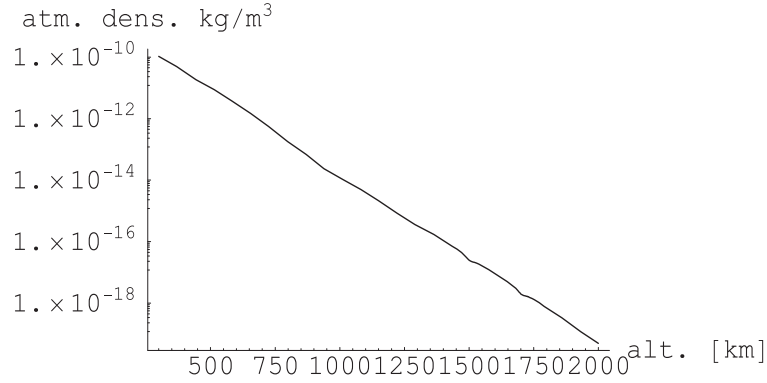


Figure 1.6 : Atmospheric mass density as a function of altitude. The atmospheric mass density is the product of average ion mass [kg] and neutral particle density [m^{-3}]. We use Mathematica to perform numerical interpolation and integration in (1.1). Altitudes beyond 2000 km are neglected.

The spacecraft has boosters burning monopropellant fuel. The exhaust velocity is

$$v_e = 2452.5 \text{ m/s}$$

The total mission consists of 9125 orbits, thus the mass of fuel required computes as

$$m = \frac{83.1608 \cdot 9125}{2452.5} \text{ kg} = 309.416 \text{ kg}$$

1.3.2 Surface charging

We are interested in the potential difference ϕ of the surface of the spacecraft and the environment while the spacecraft has an altitude in the range of 300 – 2000 km.

We assume the spacecraft has a conducting surface. Since the positive ions are considerably slower than the spacecraft itself, Kirchhoff's law states

$$A_{\text{ram}} i_p(h) + A_{\text{sc}} i_e(h) = 0 \quad (1.2)$$

where $A_{\text{ram}} = 4\text{m}^2$ is the effective area of the main body facing the ram direction, and $A_{\text{sc}} = 19\text{m}^2$ is the total area of the main body. Attached to the main body of the spacecraft is the huge solar array, which we consider to be insulated from the main body.

The value $i_p(h)$ in (1.2) refers to the ion ram saturation current density with unit $\frac{\text{A}}{\text{m}^2}$. We assume the electron current density to be of the form

$$i_e(h) = \frac{-e}{4} F(h) \exp \frac{e\phi(h)}{kT(h)}$$

where $F(h)$ is the electron thermal particle flux [$\text{m}^{-2}\text{s}^{-1}$], e is the charge of a single electron, k is the Boltzmann constant, and $T(h)$ is the electron temperature [K].

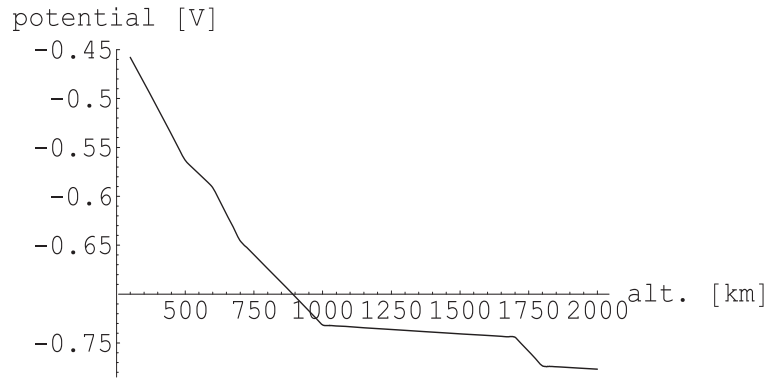


Figure 1.7 : Potential difference of the surface of the spacecraft and the environment in the LEO altitudes.

Then, the potential difference can be isolated from (1.2) as

$$\phi(h) = \frac{kT(h) \log \left(\frac{4A_{\text{ram}} i_p(h)}{eF(h)A_{\text{sc}}} \right)}{e} = 86.173 \cdot 10^{-6} \cdot T(h) \log 5.256 \cdot 10^{18} \cdot \frac{i_p(h)}{F(h)}$$

The resulting function $\phi(h)$ is plotted in Figure 1.7. The functions $T(h)$, $F(h)$, $i_p(h)$ are illustrated on the next page. We conclude that the potential difference does not exceed an amplitude of 1V. Thus, charging is not an issue in altitudes of 300 – 2000 km.

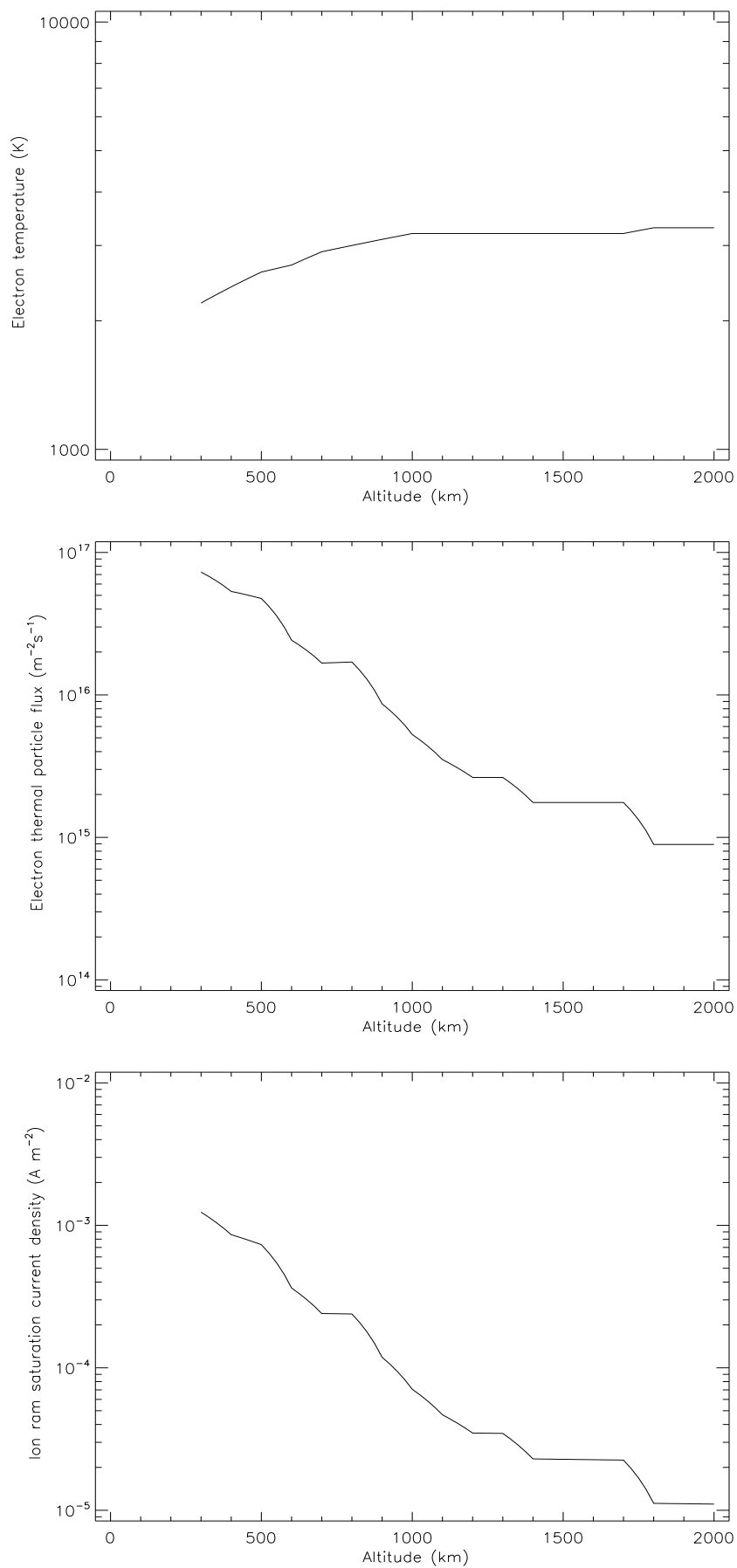


Figure 1.8 : The electron temperature $T(h)$, the electron thermal particle flux $F(h)$, and the ion ram saturation current density $i_p(h)$.

Chapter 2

Effects of radiation

2.1 Flux of particles

The radiation environment is tightly linked with the solar activity. Therefore the altitudes for the radiation belt are shifting. The models of SPENVIS are therefore simulate based on the average or on the maximum solar activities depending on the choice of the user.

All charged particles are classified into two species, positively charged ions, and negatively charged electrons. They have different density and thermal velocity distributions depending on the altitude. In general, at lower altitudes like in the ionosphere charged particles are of high density but with low energy levels compared to that ones in higher altitudes. The sun ionizes the molecules and neutral atoms, which gives the electrons and ions not quite sufficient energy to penetrate a spacecraft or even charge a spacecraft.

The spacecraft on the Pichler-Hakenberg orbit passes briefly through LEO altitudes ranging from 100 – 1000 km. As long as the spacecraft travels within the low altitude region but not in the auroral region there is the least influence due to radiation.

When the spacecraft travels in higher altitudes it traverses the inner van-Allen radiation belt. The belt is defined by the peak flux of the charged particles encountered closer to Earth as seen in Figure 2.1.

To visualize where particles above the energy levels of 0.1, 1 and 3 MeV respectively are encountered during one orbit, simulation by SPENVIS are performed for each type, electrons and protons. These energy levels are compared with the graphs of Figure 2.1 to determine the altitude. The perigee and apogee are easily determined by the regions of small and far distances between the points, which follow each other in constant time intervals.

Increasing the threshold energy levels for the particles, reveals the energy levels passed by the spacecraft by looking at Figures 2.2 – 2.5.

As indicated by Figure 2.1, the electron and proton fluxes differ in distribution according to altitude and latitude.

In the auroral region above an energy level of 0.1MeV, the electron flux dominates over the proton flux. Just beyond the auroral region, there is only minor fluxes, which indicate the low Earth neutral environment passage. In Figure 1.5, the spacecraft on its descending path passes over range of about 50 degrees of latitude below 1000 km, which is equivalent to the low Earth orbit region. Only a small fraction of 50 deg are within the auroral region. But the results for the electron flux show in all the graphs a wide range in which the spacecraft encounters energetic

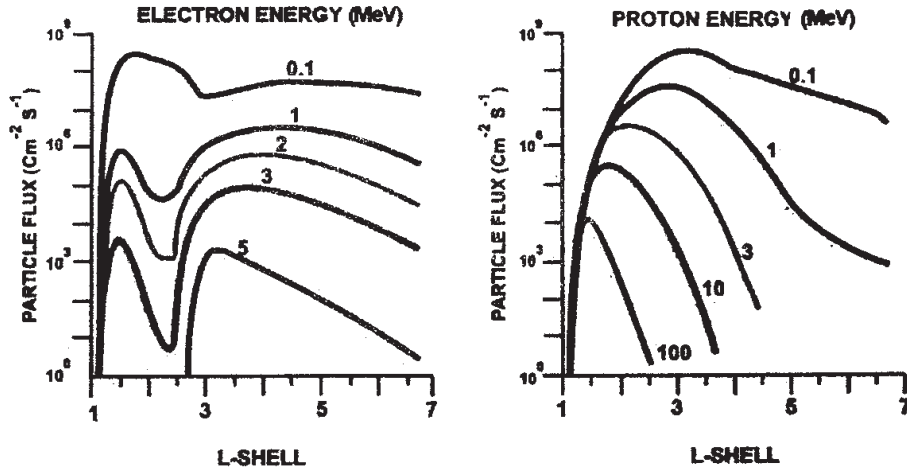


Figure 2.1 : Typical electron and proton fluxes as functions of L-values in the radiation belts. The electrons form two humps while the ions only one. The L-value is a measure of distance from the center of the Earth. It is defined as $L = 1/\cos^2\Lambda$ where Λ is the magnetic latitude (also called invariant latitude). In the equatorial region, L is a rough approximation of the Earth radius R_E , especially near the earth. The illustration has been scanned from [La07]

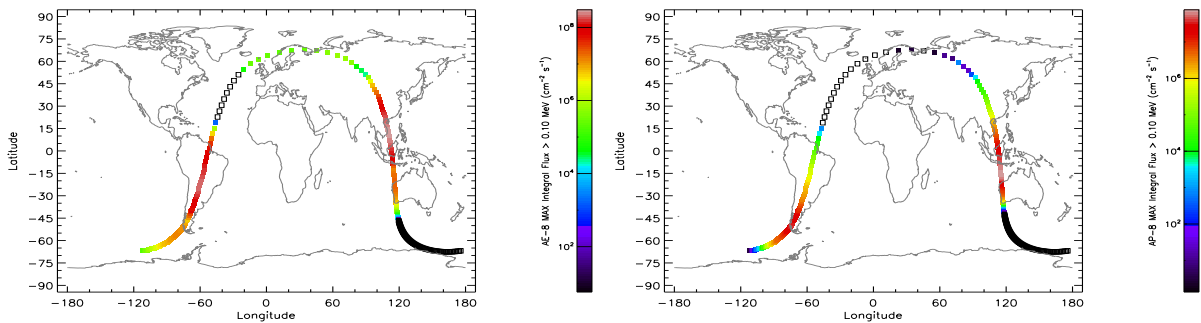


Figure 2.2 : World map of trapped electrons (left) and trapped protons (right) at energy levels above 0.1MeV [Source: SPENVIS]

electrons transported down to low altitudes.

The auroral region is of circular shape. In Figure 2.5 for electron flux greater than $5MeV \cdot cm^{-2} \cdot s^{-1}$ the region where it reaches low altitude is only from 55 – 65 deg latitude and so there is an intersection of the flux on the spacecraft orbit path between 65 – 67,5 deg latitude.

The critical phases in the mission are primarily the passages through the inner van-Allen radiation belt and secondary the passage through the auroral region at every orbit. To identify the region where the spacecraft absorbs the greatest doses of radiation we consult Figure 2.5, which holds the most significant values.

On the descending path the spacecraft crosses the inner radiation belt between 63 – 43 deg

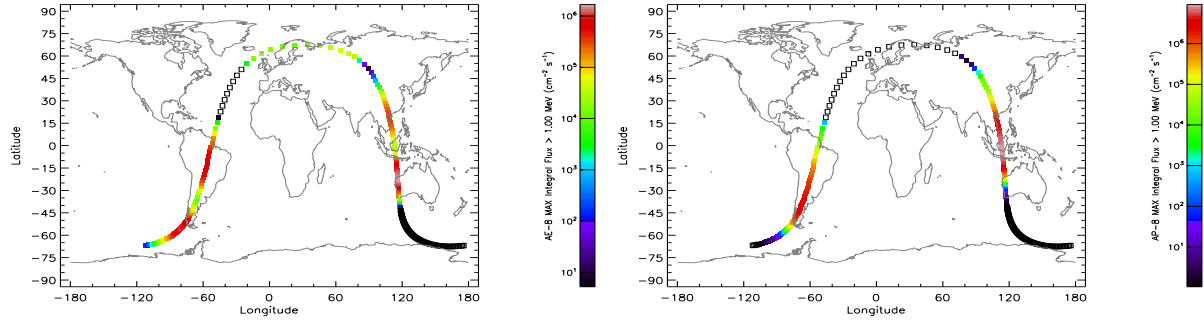


Figure 2.3 : World map of trapped electrons (left) and trapped protons (right) at energy levels above 1MeV [Source: SPENVIS]

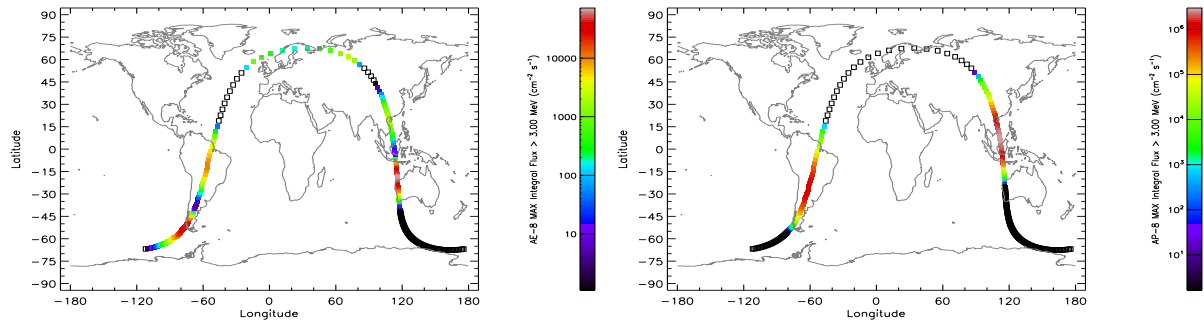


Figure 2.4 : World map of trapped electrons (left) and trapped protons (right) at energy levels above 3MeV [Source: SPENVIS]

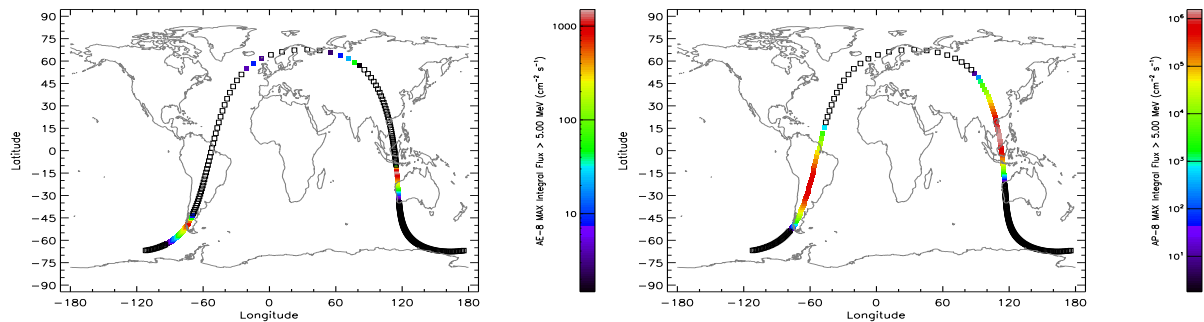


Figure 2.5 : World map of trapped electrons (left) and trapped protons (right) at energy levels above 5MeV [Source: SPENVIS]

latitude south, which indicates the layer for the electron flux over $5 \frac{\text{MeV}}{\text{cm}^2 \text{s}}$ between the altitudes of 10700 – 6200km.

On the ascending path the spacecraft crosses the radiation belt between 10 – 32 deg at altitudes

9100 – 13400km.

For the descending and the ascending path there must be different values because of the inclination of the orbit in combination with the argument of perigee.

The plot of the electron flux of energy levels $> 3MeVcm^{-2}s^{-1}$, see Figure 2.4, confirms the graph in Figure 2.1 and shows for the specific flux at certain altitude according to the latitude, where the spacecraft moving on its orbit crosses the borders of the radiation belt layers. Both, for the electrons and for the protons there are two layers. For this statement, values expressed in terms of the given orbit are summed up in Figure 2.6.

Electron Flux		descending				ascending			
e-Flux	entry Latitude	leaving latitude	entry altitude	leaving altitude	entry Latitude	leaving latitude	entry altitude	leaving altitude	
MeV cm ⁻² s ⁻¹	[°]	[°]	[km]	[km]	[°]	[°]	[km]	[km]	
upper	>3	-67	-40	13200	5700	0	-38	7300	14300
lower	>3	-40	15	5700	1150	42	0	2450	7300

Proton Flux		descending				ascending			
p-Flux	entry Latitude	leaving latitude	entry altitude	leaving altitude	entry Latitude	leaving latitude	entry altitude	leaving altitude	
MeV cm ⁻² s ⁻¹	[°]	[°]	[km]	[km]	[°]	[°]	[km]	[km]	
>3	-58	13	9200	1100	48	-27	1900	12300	

Figure 2.6 : Latitudes and altitudes where the spacecraft crosses the borders of the inner radiation belt for particle fluxes above $3MeVcm^{-2}s^{-1}$. The indication upper and lower refers to the layers of electron flux defined from one minimum flux to another while one is higher and one is lower in altitude like in Figure(2.1). [Source: SPENVIS]

The averaged spectra in Figure 2.7 gives an idea how common certain energy levels for electron are. In addition, the averaged spectra in Figure 2.8 gives an idea how common certain energy levels for protons are.

2.2 Lifetime and performance degradation

This section deals with protective measurements for the solar arrays, as well as the memory device that are onboard the spacecraft.

In addition, we calculate the erosion of a silver plate due to atomic oxygen. The plate is crucial to carry out a classified scientific experiment.

2.2.1 Shielding of the solar array

We aim to devise shielding for the solar arrays, to limit the fluence of electrons reaching the solar arrays to

$$F = 10^{15} \frac{\text{electrons}}{\text{cm}^2}$$

during the entire mission.

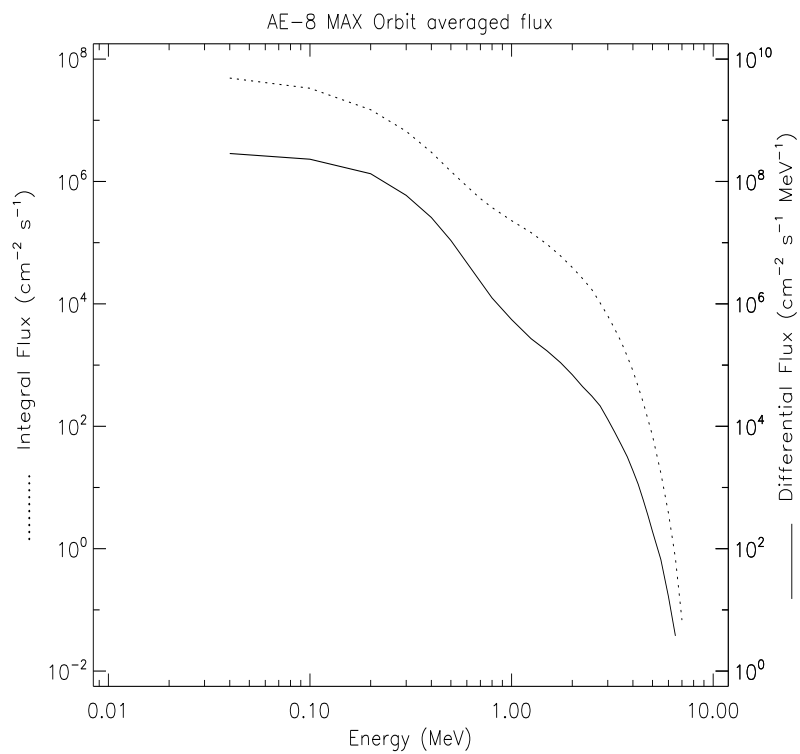


Figure 2.7 : Averaged spectra of trapped protons of all Flux above $0.1 \text{ MeV cm}^{-2} \text{ s}^{-1}$ [Source: SPENVIS]

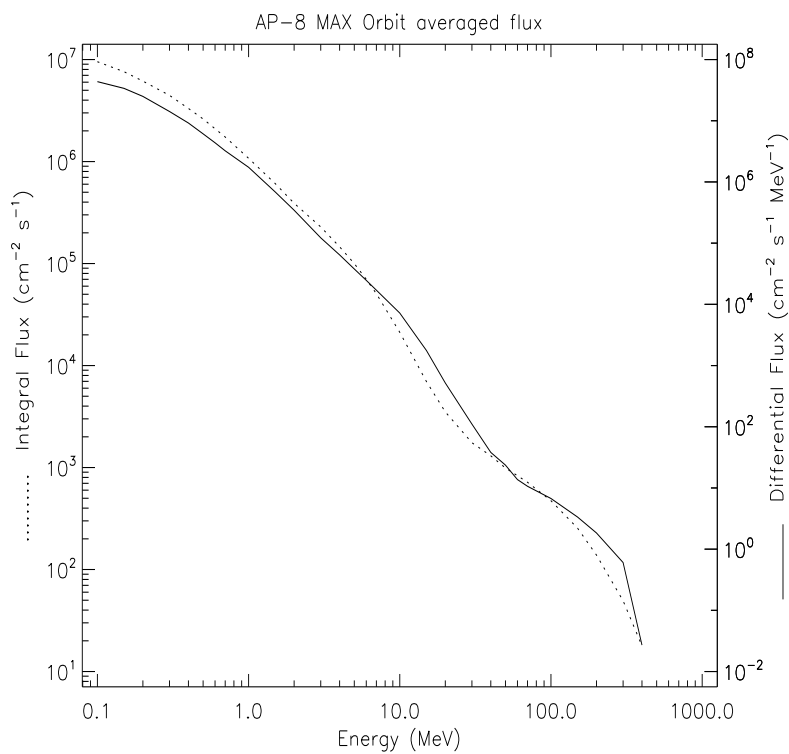


Figure 2.8 : Averaged spectra of trapped protons of all Flux above $0.1 \text{ MeV cm}^{-2} \text{ s}^{-1}$ [Source: SPENVIS]

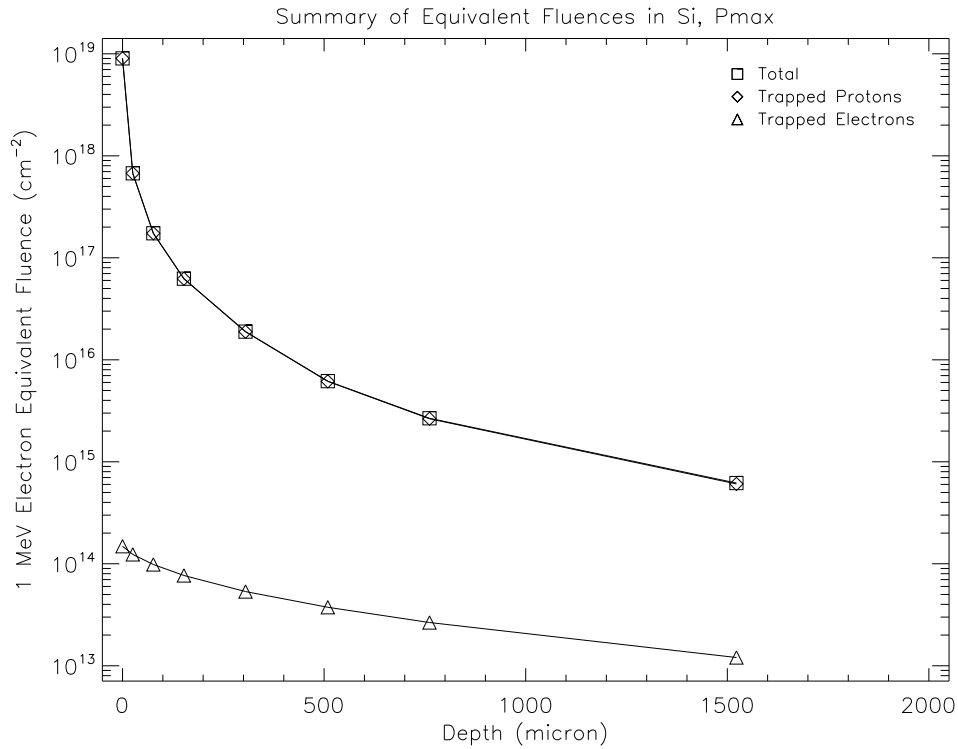


Figure 2.9 : 1MeV electron equivalent fluence penetrating the protective layer of silicium as a function of shielding thickness.

As protective shielding, we cover the solar arrays by a layer of glass. We consider the covering glass to have the same shielding properties as silicium. Then, SPENVIS allows us to simulate the 1MeV electron equivalent fluence with respect to P_{\max} .

Figure 2.9 shows that a thickness of the protective layer as

$$x = 1270\mu\text{m} = 1.27\text{mm}$$

reduces the electron equivalent fluence to the desired limit. However, assuming that our satellite is equipped by an overall area of $A = 16\text{m}^2$ solar cells, this covering layer has a mass of

$$m_{\text{cover}} = \rho_{\text{Si}}xA = 2.55 \cdot 1.27 \cdot 16 \text{ kg} = 40.8 \text{ kg}.$$

Therefore, the estimated thickness of the layer of glass is not reasonable to be used in our mission.

2.2.2 Total dose in the memory device

The semi-conductor memory device is made mainly out of silicon. The device withstands 1Mrad of radiation before it ceases functioning. It is mounted on the front face of the spacecraft in a box with shielding of 1mm.

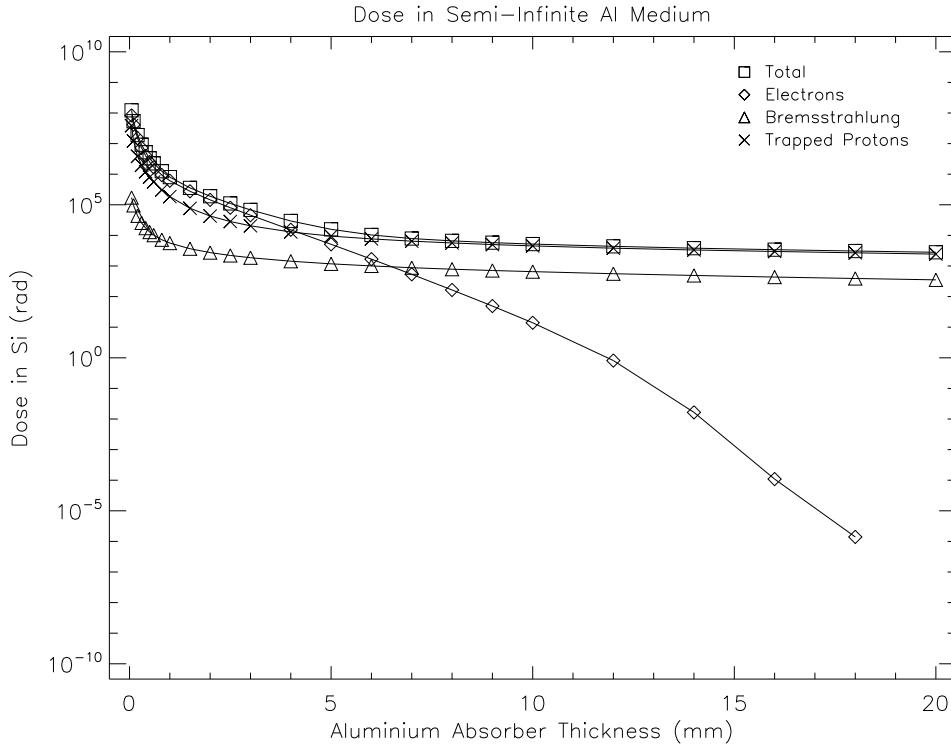


Figure 2.10 : Radiation dose perceived during 5 years in orbit as a function of shielding thickness.

SPENVIS simulates the radiation dose perceived during the entire mission. The results are plotted in Figure 2.10. For a shielding of 1mm, we yield 1Mrad dose absorbed during 5 years in orbit.

Employing a safety margin of 10%, we recommend to use a shielding of 1.1mm. This should ensure the device to function during the entire mission.

2.2.3 Atomic oxygen erosion

For a classified scientific experiment, there is a flat silver plate mounted on the spacecraft. The normal of the surface of the plate points in ram direction.

According to [Ej07b], the reactivity of silver due to atomic oxygen is

$$\text{RE}_{\text{Ag}} = 1.05e - 23 \frac{\text{cm}^3}{\text{atom}}$$

The thickness of silver x eroded due to atomic oxygen during time τ is determined by the integral

$$x = \int_0^\tau \text{RE}_{\text{Ag}} n(t) v(t) dt = m \int_0^T \text{RE}_{\text{Ag}} n(t) v(t) dt$$

where $n(t)$ is the number density of atomic oxygen, and $v(t)$ is the velocity of the spacecraft. To simplify the numerical integration, we consider the time $\tau = mT$ to be an integral number of

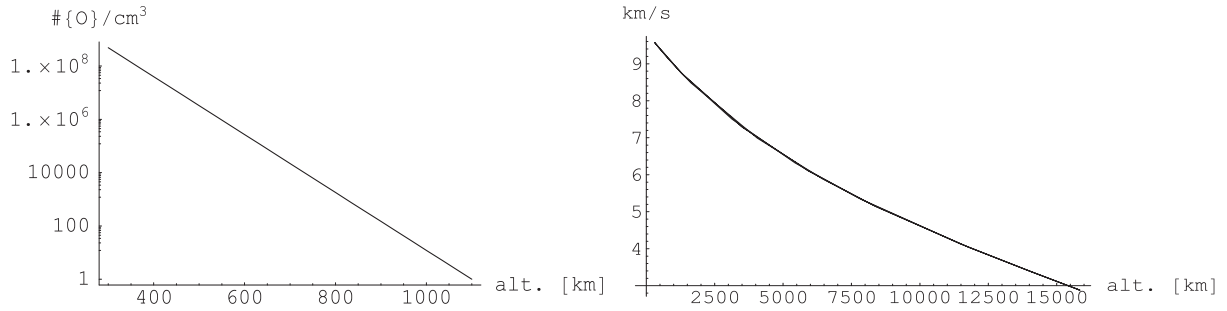


Figure 2.11 : On the left, we show the quantity of atomic oxygen $n(h)$ relative to the altitude. To the right, we plot the velocity $v(h)$ relative to the altitude.

$m \in \mathbb{Z}$ orbits with period $T = 17232.8s$. The erosion effect during one orbit is then extrapolated to m orbits.

We model the number density of atomic oxygen as a function of altitude h [km] as

$$n(h) = \exp\left(\frac{1100 \text{ km} - h}{40 \text{ km}}\right)$$

As the Figure 2.11 shows that $n(h)$ gives an excellent approximation to the curve plotted in [Ej07b].

Using Mathematica, we yield the erosion effect during one orbit as

$$\int_0^T \text{RE}_{\text{Ag}} n(t) v(t) dt = 0.00926741 \mu\text{m}$$

This corresponds to $x = 84.56 \mu\text{m}$ during the entire mission.

Previous testing in a secret laboratory facility has shown, that the experiment yields meaningless results after a thickness of $x = 50 \mu\text{m}$ silver has been eroded. Therefore, the experiment should be turned off roughly after 3 years.

2.2.4 Influence of glow on optical sensor

We use protective shielding on the surface of the spacecraft. In the neutral environment, i.e. in low altitudes the glow phenomenon will occur.

From [Ej07b], we know that the brightness of the spacecraft glow is estimated from the altitude h [km] as

$$g(h) = \frac{1}{4\pi} 10^{10} \exp(7 - 0.0129h)$$

Onboard the spacecraft, we have a CCD array with an ultra amplifying optical system. During operation mode, the instrument is pointing into deep space. There is a danger of damaging the CCD array when exposed by more than $10^6 \frac{\text{photons}}{\text{cm}^2 \text{ s sr}}$ for several seconds. Figure 2.12 shows, that the instrument requires coverage during the flight through the auroral regions.

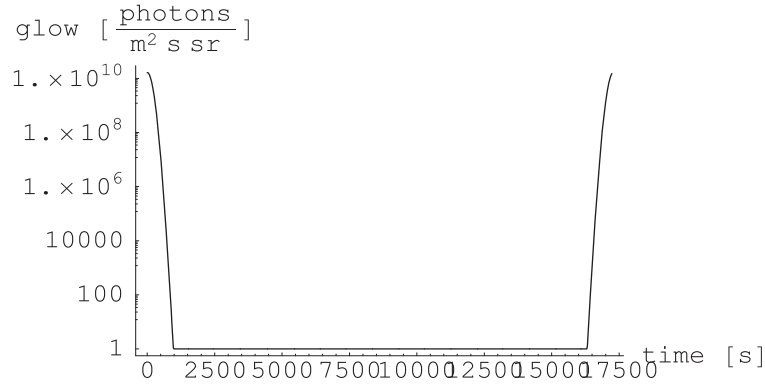


Figure 2.12 : Strength of glow during one orbit. Values below $1 \frac{\text{photons}}{\text{m}^2 \text{ s sr}}$ are neglected.

2.3 Single event upset

A single event upset (SEU) is a change of state in a semiconductor device caused by an intruding high-energy particle.

With respect to the particle flux encountered in the Pichler-Hakenberg orbit, we investigate the SEU rate for different choices of on-board volatile memory, such as nmos2164, CMOS R160-25, Bipolar 93L422, and SMJ329C50.

We favor the device with the lowest SEU rate, which turns out to be the CMOS R160-25 memory.

2.3.1 LET spectrum

To estimate the SEU rate, we assume a shielding thickness of $1\text{g}/\text{cm}^2$ (Aluminium equivalent). We consider the maximum ion range from hydrogen to uranium. The simulation is carried out under peak composite worst-case flare flux and worst-case composition, taking trapped protons into account.

Having specified this environment, SPENVIS provides the total mission differential flux $f(L)$ for values of the linear energy transfer in the range of $L \in (1.6943, 104200) [\frac{\text{MeV cm}^2}{\text{g}}]$. The function $f(L)$ characteristic for the Pichler-Hakenberg orbit is shown in Figure 2.14.

2.3.2 Cross section and components characteristics

We model the influence of the LET value on the SEU rate as a Weibull distribution function. That is, we assume the sensitivity function $\sigma : \mathbb{R}_0^+ \rightarrow \mathbb{R}$ is of the form

$$L \mapsto \begin{cases} 0 & L \leq L_0 \\ C_s(1 - \exp[-(\frac{L-L_0}{W})^s]) & L > L_0 \end{cases} \quad (2.1)$$

The four parameters L_0, C_s, W, s depend on the specific material. The values corresponding to several of the devices are stated in [Ke04a] as

Device	L_0 [$\frac{\text{MeV cm}^2}{\text{mg}}$]	C_s [cm^2]	W [$\frac{\text{MeV cm}^2}{\text{mg}}$]	s
nmos2164	0.487	1.71e-5	4.95	1.422
CMOS R160-25	136.8	1.2e-5	350	3.0
Bipolar 93L422	0.6	2.6e-5	4.4	0.7

Sensitivity of SMJ329C50GFAM66

The mono-beam experimental results of the SMJ329C50GFAM66 component are stated in [Ke04a]. Employing a least-square fit to the data points, we obtain the following constants to be used in (2.1)

$$\begin{aligned}
 L_0 &= 0.9901 && \frac{\text{MeV cm}^2}{\text{mg}} \\
 C_s &= 5.7322e - 6 && \text{cm}^2 \\
 W &= 4.9898 && \frac{\text{MeV cm}^2}{\text{mg}} \\
 s &= 0.9888
 \end{aligned}$$

Figure 2.13 shows both, the data points as well as the function $\sigma(L)$ with the parameters stated above. The following MATLAB code has been developed to perform the least-square fit.

```

function x=smj
% code approximates coefficients of the weibull distribution
% function describing the sensitivity of the SMJ329C50GFAM66

data=[
% MeV    LET      n/(F*t)
0.6      3.497    1.0667e-9
0.72     3.255    9.9960e-7
9.6      0.487    3.0019e-6
4.8      1.413    4.7031e-6
20       2.239    4.9000e-6
56       3.398    4.9985e-6
84       6.131    5.0052e-6
786      7.286    5.0119e-6];

x=abs(lsqcurvefit(@weibull,[3e-4 5 1 1],data(:,2),data(:,3)));

clf reset;
plot(data(:,2),data(:,3),'r*'); hold on;
xdata=linspace(0,10,100);
plot(xdata,weibull(x,xdata));
xlabel('LET [MeV cm^2/mg]')
ylabel('\sigma(LET) [cm^2]')
grid on

```

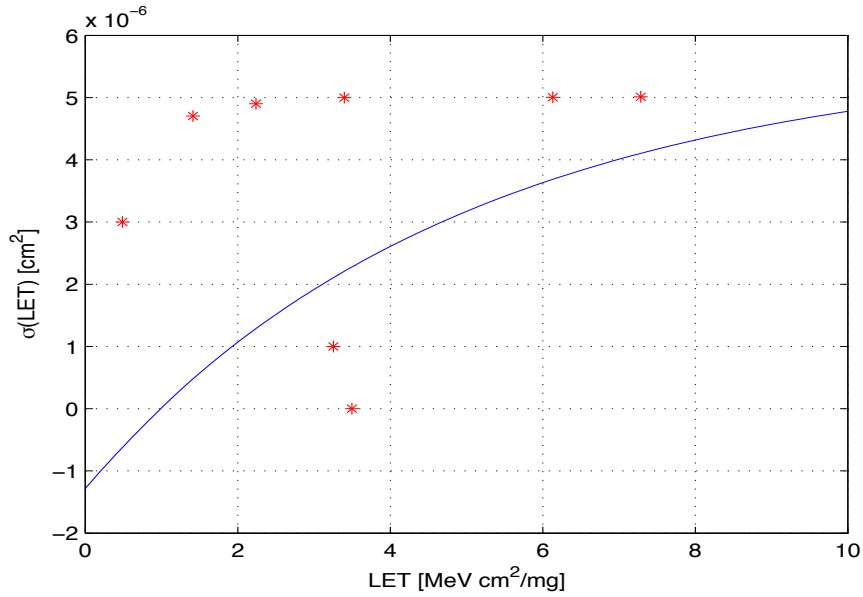


Figure 2.13 : Approximation result for the sensitivity of the SMJ329C50GFAM66. The red dots represent the data points derived from Table 4 in [Ke04a].

```
function y=weibull(x,xdata)
    y=x(1)*(1-exp(-((xdata-x(4))/x(2)).^x(3))));
```

2.3.3 SEU rate estimation

[Ke04a] provides the guideline to compute the single event upset rate ρ . The SEU rate is the value of the following integral

$$\rho = \int_0^{\infty} f(L)\sigma(L)dL \quad (2.2)$$

where $f : \mathbb{R}_0^+ \rightarrow \mathbb{R}$ is the differential flux with respect to the linear energy transfer, and $\sigma : \mathbb{R}_0^+ \rightarrow \mathbb{R}$ is the sensitivity function of a specific material.

Recall that the sensitivity function $\sigma(L)$ stated in (2.1) is determined by the four parameters

$$L_0, C_s, W, s$$

that depend on the specific material. The corresponding values are taken from [Ke04a]. Concerning the SMJ329C50 device, we have estimated appropriate values in Subsection 2.3.2.

Using numerical integration, we obtain a good approximation of the SEU rate ρ as defined in (2.2) for all four devices.

Device	L_0 [$\frac{\text{MeV cm}^2}{\text{mg}}$]	C_s [cm^2]	W [$\frac{\text{MeV cm}^2}{\text{mg}}$]	s	SEU rate
nmos2164	0.487	1.71e-5	4.95	1.422	0.0958
CMOS R160-25	136.8	1.2e-5	350	3.0	6.1961e-5
Bipolar 93L422	0.6	2.6e-5	4.4	0.7	0.1463
SMJ329C50GFAM66	0.9901	5.7322e-6	4.9898	0.9888	0.0308

Radiation causes the least number of single event upsets in the CMOS R160-25 device, which we therefore recommend to incorporate in the design of the satellite.

The SEU rates ρ are yielded using the MATLAB code below. The numerical approximation of the differential flux $f(L)$ provided by SPENVIS is not included.

```
function z=seu
% numerical integration of the product sigma(LET)*flux(LET)
% for four different devices

let
x=LETdat(:,1);
Y=LETdat(:,3);
z=[];

for n=1:4
switch n
case 1
Ln=0.487; Cs=1.71e-5; W=4.95; s=1.422;
case 2
Ln=136.8; Cs=1.2e-5; W=350; s=3.0;
case 3
Ln=0.6; Cs=2.6e-5; W=4.4; s=0.7;
case 4
Ln=0.9901; Cs=5.7322e-6; W=4.9898; s=0.9888;
end
y=Cs*(1-exp(-((x-Ln)/W).^s)).*(x>Ln)*0.0001;
z=[z trapz(x,y.*LETdat(:,3))];
Y=[Y y];
end

loglog(repmat(x,[1 5]),Y);
legend({'LET spectrum','nmos2164','CMOS R160-25','Bipolar 93L422','SMJ329C50'})
xlabel('LET [MeV cm^2/mg]')
```

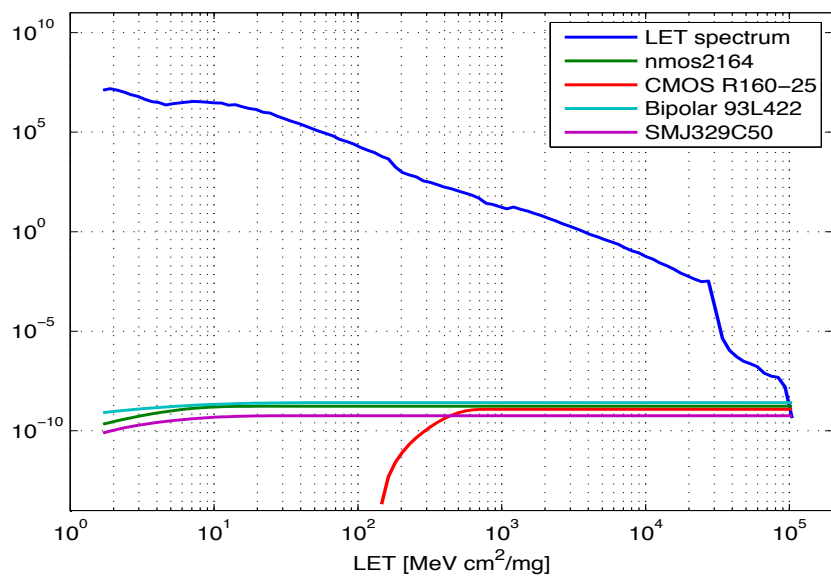


Figure 2.14 : On the logarithmic scale, we plot the sensitivity function $\sigma(L)$ [cm²] for all four materials, as well as the differential flux $f(L)$ labeled as LET spectrum.

Conclusion

The spacecraft on the Pichler-Hakenberg orbit traverses the auroral region, the neutral environment in the LEO region, and encounters high energetic radiation in the inner van-Allen radiation belt. There are a lot of accumulating environmental effects.

The particle flux varies in density over the geomagnetic latitude and altitude. The expected effects of environmental flux from the radiation belts match the simulation.

To compensate the drag encountered in the low altitudes, we require 310 kg of mono-propellant fuel.

The potential difference in altitudes below 2000 km does not exceed an amplitude of 1V. Thus, charging is not an issue in these altitudes.

A layer of thickness of 1.27 mm to protect the solar arrays reduces the electron equivalent fluence to the desired limit. However, employing such a covering layer contributes significantly to the total mass.

To protect the memory device, we recommend to use a shielding of 1.1mm. This should ensure the device to function during the entire mission.

The silver plate mounted in the front of the spacecraft will be eroded due to atomic oxygen by 84.56 μm during the mission.

The sensitive CCD sensor requires coverage during the passage of the auroral region to shield from glow.

Employing a least-square fit to the experimental data points of the SMJ329C50GFAM66 component, we obtain the following parameters that define the Weibull distribution function

$$\begin{aligned}
 L_0 &= 0.9901 && \frac{\text{MeV cm}^2}{\text{mg}} \\
 C_s &= 5.7322e - 6 && \text{cm}^2 \\
 W &= 4.9898 && \frac{\text{MeV cm}^2}{\text{mg}} \\
 s &= 0.9888
 \end{aligned}$$

Radiation causes the least number of single event upsets in the CMOS R160-25 device, which we therefore recommend to incorporate in the design of the satellite as semi-conductor memory device.

Bibliography

- [ESA07] ESA: *The Space Environment Information System*, 2007
<http://www.spennis.oma.be/spennis/>
- [Ej07a] Ejemalm, Johnny: *Slides from the Space Environment lecture*, 2007
- [Ej07b] Ejemalm, Johnny: *Space-Environment Interaction • Exercise 1-6*, 2007
- [Ke04a] J. Keno: *Space Environment Laboratory Work with SPENVIS: Radiation Environment and Effects*, Department of Space Science, Lulea, 2004
- [Ke04b] J. Keno: *SPENVIS Brief Guideline*, Department of Space Science, Lulea, 2004
- [La07] S. Lai: *The Earth's Space Plasma Environment*, Lecture notes, 2007
- [WiRb07] *Van Allen radiation belt*, Wikipedia 2007
http://en.wikipedia.org/wiki/Van_Allen_radiation_belt

Abbreviations

eV	Electron Volt = $1.602 \cdot 10^{-19}C$
LET	Linear Energy Transfer (\approx Stopping power)
LEO	Low Earth Orbit, range of altitude 100km – 1000km
SPENVIS	SPace ENViroment Information System
SEL	Single Event Latch-up
SEU	Single Event Upset